Modeling Chromate Ion-Exchange Processes

In spite of chromate's very high selectivity at acidic pH, fixed-bed chromate-exchange processes always suffer from severe gradual breakthroughs of chromate during column runs. Earlier, Sengupta and Clifford confirmed that such a gradual breakthrough is an equilibrium phenomenon and provided the underlying ion-exchange mechanism. An algorithm, developed with the aid of the governing chromate ion-exchange mechanism, is presented here to predict the salient properties of chromate-exchange processes in a multicomponent system. The model predicts the gradual chromate breakthroughs during column runs fairly accurately and also accounts for other unusual characteristics of chromate ion exchange. Average separation factor models, often used for designing fixed-bed ion-exchange processes, are unable to predict the gradual breakthrough characteristics of a preferred component such as chromate.

Arup K. Sengupta
Environmental Engineering Program
Lehigh University

Lois Lim
Chemical Engineering Department
Fritz Engineering Lab 13
Lehigh University
Bethlehem, PA 18015

Introduction

The presence of potentially toxic hexavalent chromate in various industrial wastewaters is always a major pollution threat and several researchers have investigated the potential application of anion-exchange processes for chromate's selective removal and possible receovery from chromate-laden wastewaters (Kunin, 1976; Newman and Reed, 1980; Yamamoto et al., 1975; Richardson et al., 1968). In general, all these investigators have confirmed the viability of the chromate-exchange process at acidic pH despite severe competition from competing chloride and sulfate ions, which may be present in wastewaters in concentrations several orders of magnitude greater than chromate. Such a viability is primarily due to chromate's very high selectivity for anion-exchange resins over other competing ions. The regeneration process has also been found to be highly efficient for both weakly basic and strongly basic anion resins (Kunin, 1976; Newman and Reed, 1980), sodium hydroxide and alkaline brine being the most commonly used regenerant chemicals.

However, in spite of very high selectivity of chromate anions for commercial organic anion-exchange resins at slightly acidic pH (3.0–6.0), fixed-bed chromate-exchange processes suffer from severe gradual breakthrough of chromate during column operations, as shown later in Figure 6. The phenomenon of chromate's gradual breakthrough has been observed for all types of anion-exchange resins and also in the presence of different competing ions, namely, sulfate, chloride, and nitrate. For a highly preferred species such as chromate, such a gradual breakthrough is counterintuitive and is not caused by poor diffusion-controlled kinetics. Sengupta and Clifford (1986) have systematically shown that such a gradual breakthrough is an equilibrium property of chromate ion exchange and stems primarily from chromate's ability to dimerize inside the anion exchange resins.

The primary objective of this paper is to demonstrate how knowledge of the chromate ion-exchange mechanism at acidic pH may be used to develop a design algorithm to predict its fixed-bed column behavior in a multicomponent system, where chromate is the most preferred species but present at concentrations several orders of magnitude lower than the concentrations of competing anions. The phenomenon of gradual breakthrough for a preferred species like chromate is unique and cannot be dealt with by constant separation factor models, even though such models have been used effectively by Clifford (1982), Wang and Huang (1983), and Yu and Wang (1986) for other ion-exchange processes. Since chromate is a toxic substance, the length of the column run is always determined by some predetermined chromate concentration in the effluent as dictated by regulatory agencies. It will be shown in this communication how the lengths of the column runs, in many cases, may be independent of the influent chromate concentrations.

Since the chromate ion-exchange mechanism will form the basis of this presentation, a brief summary of the salient properties of chromate ion exchange along with speciation of various chromate anions is provided below.

1. Chromates may exist in the aqueous phase in different ionic forms, with total chromate and pH dictating which particular chromate species will predominate. For convenience in discussion, we will describe the total chromate species as Cr(VI) or chromate, while each individual species will be represented by

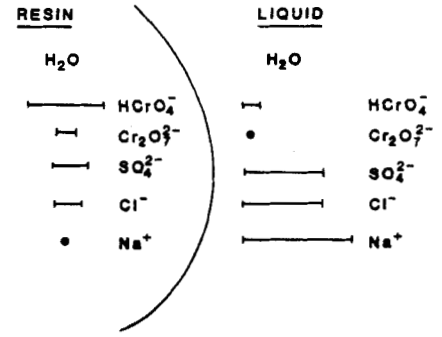

Figure 1. Qualitative distribution of counterions and co-ion (sodium) during chromate ion exchange.

its chemical formula. The following are the important equilibrium reactions for different Cr(VI) species (Butler, 1967; Tong and King, 1953). The log of the equilibrium constant, K, in each reaction is also given.

Reaction	log K (25°)	
$H_2CrO_4 \rightleftharpoons H^+ + HCrO_4^-$	−0.8	(1)
$HCrO_4^- \rightleftharpoons H^+ + CrO_4^{2-}$	−6.5	(2)
$2HrCrO_4^- \rightleftharpoons Cr_2O_7^{2-} + H_2O$	1.52	(3)

At slightly acidic pH (below 6.5), $HCrO_4^-$ is the most predominant Cr(VI) species in the aqueous phase while $Cr_2O_7^{2-}$ is practically absent for normally encountered chromate-laden wastewates with total chromate concentration less than 100 mg/L. However, during chromate ion exchange at acidic pH, $Cr_2O_7^{2-}$ is significantly present inside the ion exchanger. This phenomenon may be viewed as a resin-phase dimerization of $HCrO_4^-$ into $Cr_2O_7^{2-}$ in accordance with reaction 3 and may be predicted by the Donnan membrane principle. Figure 1 illustrates the chromate ion-exchange mechanism.

2. In spite of chromate's very high selectivity, the binary chromate isotherms at acidic pH are always an unfavorable type, that is, concave upward at low chromate concentrations. Such unfavorable characteristics are inherent properties of chromate ion exchange and are independent of the types of ion-exchange resins and competing anions. Distribution of chromate between the exchanger and the aqueous phases, when chromate is a trace species, is given by

$$y_{Cr} = A_1 x_{Cr} + A_2 x_{Cr}^2 \tag{4}$$

where y_{Cr} and x_{Cr} represent equivalent fractions of Cr(VI) in the exchanger phase and aqueous phase, respectively, and A_1 and A_2 are constants which depend on the type of anion-exchange resin used, total concentration of the competing anions, various equilibrium constants, and other factors. The appendix provides the derivation of Eq. (4), which has a positive curvature, that is,

$$\frac{\partial^2 y_{Cr}}{\partial x_{Cr}^2} > 0 \tag{5}$$

Such an unfavorable characteristic of chromate anion exchange is an equilibrium property and is responsible for gradual breakthrough of chromate during fixed-bed column runs.

3. At acidic pH, unfavorable chromate isotherms are observed only at low chromate loadings of the anion-exchange resins. With increased chromate loadings, the initial positive curvature of the chromate isotherms changes into a negative curvature (favorable characteristic) with an inflection point marking the transition between curvatures. Anion-exchange resins with polystyrene matrices are quite chromate-selective; the inflection points, therefore, often occur well within the range of chromate concentration (0–20.0 mg/L) normally encountered in various chromate-laden industrial wastewaters. Figure 2 includes the chromate-sulfate and chromate-chloride isotherms, and a change in curvature with increased chromate loading may be readily noticed. Figure 2 clearly illustrates such a change in curvature when chromate selectivity, (y_{Cr}/x_{Cr}) is plotted along the ordinate. For gas-solid adsorption, isotherms of this shape are commonly referred to as BET type V (Wankat, 1985), but they are practically unknown in liquid-solid sorption.

4. Chromates may not be the only anions to exhibit the foregoing anomalous characteristics. Other polynuclear species, namely, molybdenum and tungsten, which tend to polymerize at relatively high concentrations, as shown below, are likely to show similar ion-exchange characteristics as chromates and cause gradual breakthroughs during fixed-bed column runs.

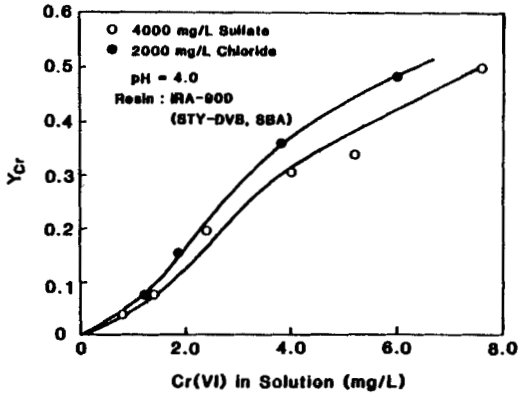

Figure 2a. Changes in curvature of chromate-chloride and chromate-sulfate isotherms with increased loadings.

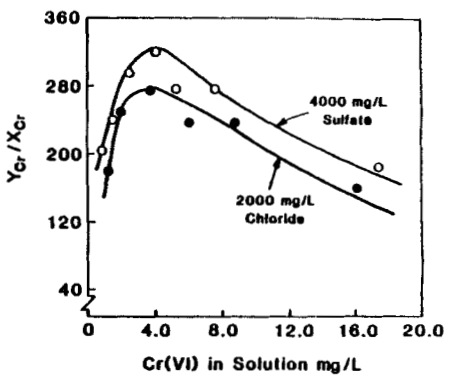

Figure 2b. Changes in chromate distribution coefficients through a maximum with increased chromate loadings.

$$7MoO_4^{2-} + 8H^+ \rightleftharpoons Mo_7O_{24}^{6-} + 4H_2O \quad (6)$$

$$6Wo_4^{2-} + 7H^+ \rightleftharpoons HW_6O_{21}^{5-} + 3H_2O \quad (7)$$

Basic Approach

A fixed-bed run is terminated when the concentration of the species to be removed reaches a predetermined value in the effluent. This time and related bed volume throughput can be predicted from a knowledge of the concentration velocity of the species in question. Any concentration velocity, v_{Ci}, for a species i is a function of the liquid velocity, v_0, and the local concentration gradient between the exchanger phase and aqueous phase

$$v_{Ci} = \left(\frac{\partial z}{\partial t}\right)_{Ci} = \frac{v_0}{1 + \left(\frac{\partial \bar{C}_i}{\partial C_i}\right)_z} \quad i = 1, \ldots, n \quad (8)$$

$\bar{C}_i$ and C_i are the exchanger phase and aqueous phase concentrations of i per unit volume of bed, respectively. Equation 8 is derived from a mass balance on species i, neglecting axial dispersion and considering only convective flux; the derivation is given by Helfferich and Klein (1970).

For an unfavorable isotherm (positive curvature) with instantaneous attainment of local equilibrium, where $\bar{C}_i$ is a unique function of C_i, the concentration velocity of i may be determined by using Eq. 8 for each individual concentration, and the increase in effluent concentration is a gradual one. For a favorable isotherm, however, the concentration step is ideally sharp, barring any mass transfer limitations, and is not covered by Eq. 8. Here the definition of the concentration velocity is not applicable and the quotient $(\partial \bar{C}_i/\partial C_i)$ does not exist. The step velocity, that is, the rate of advance of such a step between fixed concentrations of species i, is given by

$$v_{\Delta Ci} = \frac{v_0}{1 + \frac{\overline{\Delta C_i}}{\Delta C_i}} \quad (9)$$

where $\overline{\Delta C_i}$ and ΔC_i are the concentration differences between the upstream and downstream sides of the step. For a favorable isotherm, therefore, the change in concentration of i at the exit of the column is an abrupt one and is referred to as a shock. The following simplification is important in order to be able to apply Eq. 8 and 9 for predicting the effluent histories of chromate during fixed-bed column runs in a multicomponent system.

Chromate concentration is several orders of magnitude lower than that of competing sulfate and chloride; in addition, chromate is preferred by the anion-exchange resin over sulfate and chloride. As a result, the concentrations of individual competing ions remain practically the same along the length of the ion-exchange bed, even though chromate concentration is changing. This is a general characteristic of a preferred trace component in the presence of other bulk species. Therefore, for given concentrations of the competing ions, the partial derivative in the denominator of Eq. 8 for the unfavorable portion of the chromate isotherm degenerates into an ordinary derivative, $\overline{dC_i}/dC_i$, where $\bar{C}_i$ is dependent only on C_i for a fixed composition of the influent. Similarly, for the favorable portion of the chromate isotherm, the quotient $\overline{\Delta C_i}/\Delta C_i$ in Eq. 9 is dependent only on the equilibrium distribution of chromate between the exchanger phase and the aqueous phase against a constant background of other competing anions.

Other assumptions are fairly straightforward:

- Constant feed composition, that is, a single step change in the influent
- Uniform presaturation (chloride form) of resins
- Local ion exchange and dissociation equilibria and negligible mass transfer effects
- Exclusion of co-ions from the resin interior, that is, negligible electrolyte penetration
- Negligible shrinking or swelling of the resins
- Isothermal, ideal plug flow behavior
- No specific interactions other than ion exchange

Transition from gradual to shock concentration waves

Consider the isotherm in Figure 3a, where the positive curvature changes to negative with an increase in the aqueous phase chromate concentration, but at the same total concentration of the competing ions. C_{in} corresponds to the aqueous phase chromate concentration at the inflection point d. Depending on the influent chromate concentration, the following types of effluent histories are possible.

1. As long as the influent chromate concentration is equal to or less than C_{in}, only gradual breakthroughs will occur and no shocks will be present, because lower concentrations always move at faster speeds. Concentration velocity for any concentration under this condition may be determined using Eq. 8, that is, by finding the slope $\overline{dC}/dC$ of the isotherm at the concentration in question. Considering two separate column runs, with chromate feed concentrations of C_{in} in one and C_{f1} ($C_{f1} < C_{in}$) in the other, the effluent histories are presented in Figure 3b, barring

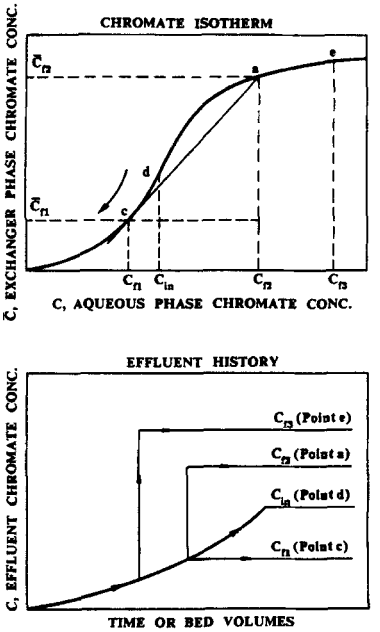

Figure 3a. Chromate isotherm showing positive curvature changing to negative at inflection point *d*.

Figure 3b. Chromate effluent histories for various feed chromate concentrations corresponding to isotherm in Figure 3a.

mass transfer limitations. Note that effluent histories up to the effluent chromate concentration of C_{f1} remain identical for both column runs, indicating that chromate concentration at the exit of the column is not influenced in this case by its influent concentration.

2. For a chromate concentration of C_{f2} (point a in the isotherm) greater than C_{in}, both gradual and shock waves will result. The transition between the two occurs at the concentration where

$$\left(\frac{d\bar{C}}{dC}\right)_{\text{gradual}} = \left(\frac{\triangle\bar{C}}{\triangle C}\right)_{\text{shock}} \tag{10a}$$

Point C (concentration C_{f1}) in Figure 3 represents such a transition point. It is obtained by drawing a tangent on the isotherm from the feed at point a, that is,

$$\left(\frac{d\bar{C}}{dC}\right)_{\text{at } C} = \frac{\bar{C}_{f2} - \bar{C}_{f1}}{C_{f2} - C_{f1}} \tag{10b}$$

Thus, there will be a gradual breakthrough first up to a chromate concentration equal to C_{f1}, followed by an abrupt transition (shock) from C_{f1} to C_{f2}. Tondeur and Bailly (1986), Golden (1972), and Tudge (1961) have provided strategies for locating such transition points with different types of isotherms. Figure 3 provides the predicted chromate effluent history for a feed concentration of C_{f2}. Again, if C_{f1} is the maximum allowable chromate concentration in the treated water at the exit of the column, the column run is to be terminated at the same time for feed concentrations anywhere between C_{f1} and C_{f2}. As the feed concentration increases, the transition point between gradual and shock waves moves downward along the isotherm in the direction of the arrow. For a feed chromate concentration of C_{f3} ($C_{f3} > C_{f2}$), the chromate effluent history is schematically presented in Figure 3.

Formulating the Design Algorithm

As indicated in Eq. 4, chromate separation factors with respect to other competing ions are not constants when chromate tends to be a trace species. This prediction is substantiated by bindary chromate-sulfate and chromate-chloride isotherm data as presented in Tables 1 and 2. These equilibrium isotherms were determined against a constant background of competing sulfate and chloride ions in concentrations several orders of magnitude greater than chromate. Tables 1 and 2 also indicate that chromate separation factors with respect to sulfate or chloride are always much greater than unity and gradually increase with an increase in aqueous phase chromate concentration, confirming the unfavorable behavior of chromate isotherms. Constant separation factor models as used earlier by Clifford (1982), Huang and Wang (1984), and Yu and Wang (1986) are, therefore, not applicable for chromate ion exchange. In order to use the binary chromate-sulfate and chromate-chloride equilibrium data for a multicomponent system (chromate-sulfate-chloride), it is assumed that the exchanger-phase activity coefficients, f_i, of all the species tend to be constant within the range of resin compositions normally encountered in such processes. Thus, the equilibrium constants, K^{I}, K^{II}, K^{I}, and K^{II}, in Eq. A9 and A10 become equivalent to corrected selectivity coefficients (Helfferich, 1961), which take into consideration activity corrections only in the aqueous phase but not in the exchanger phase. Thermodynamically, however, the corrected selectivity coefficients are more sound design parameters than separation factors, which are often used to avoid mathematical complexity in predicting column effluent histories. Granted the premises of the foregoing assumptions, the availability of binary

Table 1. Chromate-Sulfate Isotherm at pH = 4.0

Resin: IRA-900; polystyrene matrix with quaternary-amine functionality

Competing Sulfate Ion Conc.	Aqueous Phase Cr(VI) Conc. mg/L	Resin-Phase Cr(VI) Conc. meq/g	Separation Factor* $\frac{y_{Cr}x_S}{x_{Cr}y_S}$
4,000 mg/L	0.22	0.009	41.0
	0.29	0.016	55.0
	0.345	0.028	82.0
	0.465	0.04	89.0
	0.59	0.068	120.0
	0.65	0.076	122.0
	0.84	0.115	144.0
	0.863	0.14	171.0
2,000 mg/L	0.188	0.013	34.5
	0.25	0.016	32.0
	0.315	0.032	52.0
	0.38	0.041	56.0
	0.565	0.065	59.5
	0.55	0.067	62.0
	0.65	0.123	99.0
	0.62	0.15	115.0

*Chromate's preference over sulfate is indicated by the high separation factor values

Table 2. Chromate-Chloride Isotherms at pH = 4.0

Resin: IRA-900; polystyrene matrix with quaternary-amine functionality

Competing Chloride Ion Conc.	Aqueous Phase Cr(VI) Conc. mg/L	Resin-Phase Cr(VI) Conc. meq/g	Separation Factor* $\frac{y_{Cr}x_{Cl}}{x_{Cr}y_{Cl}}$
4,000 mg/L	0.30	0.007	31.0
	0.33	0.009	39.0
	0.64	0.021	45.0
	0.74	0.033	63.0
	0.78	0.035	63.0
	0.925	0.048	73.0
	1.02	0.073	100.0
	1.2	0.08	98.0
	1.32	0.109	117.0
2,000 mg/L	0.175	0.006	22.0
	0.255	0.011	29.0
	0.45	0.026	41.0
	0.42	0.029	49.0
	0.57	0 045	55.0
	0.65	0.068	73.0
	0.71	0.072	71.0
	0.825	0.094	80.0
	1.02	0.131	92.0

*Chromate's preference over chloride is indicated by the high separation factor values

chromate isotherm data, and the understanding of the chromate ion-exchange mechanism, a stepwise algorithm for predicting the chromate effluent histories in fixed-bed ion-exchange processes can be formulated, as illustrated below, in the presence of competing sulfate and chloride anions:

Step 1. This step involves estimating the lumped corrected selectivity coefficients from the binary data. Let us consider the chromate-sulfate exchange, which after applying necessary assumptions and lumping all constant terms takes the following form:

$$[\overline{RCr_T}] = \frac{(K^I f_S)^{1/2}}{f_{HCr}} \left(\frac{[\overline{R_2SO_4}]}{[SO_4^{2-}]}\right)^{1/2} \frac{[Cr(VI)]}{\gamma_1} + \frac{2K_3K^{II}f_S}{f_{Cr_2}} \frac{[\overline{R_2SO_4}]}{[SO_4^{2-}]} \frac{[Cr(VI)]^2}{\gamma_1^2} \quad (11a)$$

or

$$Z = K_1X + K_2Y \quad (11b)$$

where

$$K_1 = \frac{(K^I f_S)^{1/2}}{f_{HCr}}, \quad X = \left(\frac{[\overline{R_2SO_4}]}{[SO_4^{2-}]}\right)^{1/2} \cdot \frac{[Cr(VI)]}{\gamma_1}$$

and

$$K_2 = \frac{2K_3K^{II}f_S}{f_{Cr_2}}, \quad Y = \frac{[\overline{R_2SO_4}]}{[SO_4^{2-}]} \cdot \frac{[Cr(VI)]^2}{\gamma_1^2}$$

K_1 and K_2 will be referred to as design constants. The numerical values of vectors X, Y, and Z can be readily calculated for any given data point in the isotherm, because all individual parameters, namely, $\overline{RCr_T}$, $\overline{R_2SO_4}$, Cr(VI), SO_4^{2-} are known and the aqueous-phase activity coefficient, γ_1, is computed using the Guntelberg equation (Stumm and Morgan, 1981)

$$-\log \gamma_1 = \frac{0.5\sqrt{I}}{1+\sqrt{I}} \quad (12)$$

where I is the ionic strength of the aqueous phase. The constants K_1 and K_2 may now be determined for a set of binary chromate-sulfate isotherm data using multiple linear regression technique with the constraint that they cannot be negative.

Similarly, for chromate-chloride ion exchange, the equilibrium can be represented by

$$[\overline{RCr_T}] = \frac{K_1 f_{Cl}}{f_{HCr}} \frac{[\overline{RCl}][Cr(VI)]}{[Cl^-]} + \frac{2K^{II}K_3 f_{Cl}^2}{f_{Cr_2}} \frac{[\overline{RCl}]^2}{[Cl^-]^2}[Cr(VI)]^2 \quad (13a)$$

$$Z = K_3X + K_4Y \quad (13b)$$

The design constants K_3 and K_4 may be determined in a similar way using binary isotherm data. Note that K_1, K_2, K_3, and K_4 are constants for a particular anion-exchange resin at acidic pH (2.0–5.0) and are independent of the concentration terms.

Step 2. This step involves computing chromate distribution between the exchanger and the aqueous phase for a ternary system (chromate, chloride, sulfate) at varying concentrations of competing chloride and sulfate ions. This requires solving the following three equations of which two are nonlinear.

$$[\overline{RCr_T}] = K_1 \left(\frac{[\overline{R_2SO_4}]}{[SO_4^{2-}]}\right)^{1/2} \frac{[Cr(VI)]}{\gamma_1} + K_2 \frac{[\overline{R_2SO_4}]}{[SO_4^{2-}]} \frac{[Cr(VI)]^2}{\gamma_1^2} \quad (14)$$

$$[\overline{RCr_T}] = K_3 \frac{[RCl][Cr(VI)]}{[Cl^-]} + K_4 \frac{[\overline{RCl}]^2}{[Cl^-]^2}[Cr(VI)]^2 \quad (15)$$

and

$$Q = [\overline{RCr_T}] + [\overline{R_2SO_4}] + [RCl] \quad (16)$$

where Q is the total exchange capacity of the resin in the absence of any electrolyte penetration. For a given background concentration of competing sulfate and chloride ions, $\overline{RCr_T}$, $\overline{R_2SO_4}$, and $\overline{RCl}$ may be determined for any aqueous phase Cr(VI) concentration using a suitable algorithm for solution of nonlinear equations. Also note that the presence of any additional competing ion other than sulfate and chloride will simply increase the number of equations to be solved in this step.

Step 3. The previous step provides exchanger-phase chromate concentration, $\overline{RCr_T}$, as a function of the aqueous-phase chromate concentration, Cr(VI), for any background concentrations of competing sulfate and chloride ions. Now using a suitable interpolation algorithm, such as a cubic spline, we may express the exchanger-phase chromate concentration $\overline{RCr_T}$, as a function of its aqueous-phase concentration, Cr(VI). Subsequently, the derivative, $\overline{dC}/dC$, can be computed and plotted against Cr(VI), indicating the concentration, C_{in}, at the inflection point.

Step 4. For chromate feed concentrations less than C_{in}, concentration velocities are determined using Eq. 8, which for practical convenience is modified to incorporate the superficial liquid velocity, v_{bulk}, and also to express the mobile phase chromate concentration per unit volume of liquid. We use the following equalities

$$\text{Actual liquid velocity,} \quad v_0 = \frac{v_{bulk}}{\epsilon} \quad (17a)$$

and

$$\text{Mobile-phase concentration of component } i \text{ per unit bed volume, } C_i = \frac{\text{mass of } i \text{ in mobile phase}}{\text{volume of liquid}} \frac{\text{volume of liquid}}{\text{volume of bed}} = C_i'\epsilon \quad (17b)$$

where ϵ is the void fraction of the ion-exchange bed.

After incorporating the identities of Eqs. 17a and 17b, Eq. 8 becomes

$$v_{Ci} = \frac{v_{bulk}}{\epsilon + \frac{d\overline{C}_i}{dC_i'}} \quad (18)$$

For any feed concentration C_f greater than C_{in}, however, both diffuse and shock waves will result and the transition will always occur at a concentration lower than C_{in}. This transition concentration, C_{tran}, is determined by trial and error using the following equality

$$\left(\frac{d\bar{C}}{dC}\right)_{tran} = \frac{\bar{C}_f - \bar{C}_{tran}}{C_f - C_{tran}} \tag{19}$$

Between C_{tran} and zero, the concentration velocities are to be determined using Eq. 18, which would give a gradual breakthrough characteristic. This is followed by a shock wave, which would cause a step increase in breakthrough concentration from C_{tran} to C_f. Note that $\bar{C}_i$ denotes the concentration of i per unit volume of bed while the solid-phase concentrations were determined per unit gram of the air-dried resin. For polystyrene resin (IRA-900), 1.0 g of air-dried resin was found to occupy 3.37 mL of bed volume. Thus,

$$\bar{C}_{Cr} = \frac{\text{mg Cr}}{\text{unit volume of bed (mL)}} = \frac{\text{mg Cr}}{\text{g air-dired resin}} \frac{1}{3.37} \frac{\text{g air-dried resin}}{\text{mL of bed volume}} = q_{Cr} \frac{1}{3.37} \frac{\text{mg Cr}}{\text{mL of bed volume}} \tag{20}$$

Step 5. Breakthrough times, t_{BC}, for chromate concentrations up to C_{tran} during a column run and the corresponding bed volumes of water fed (BV) are given by

$$t_{BC} = \frac{L}{v_{Ci}} \tag{21}$$

$$BV = \frac{v_{bulk}}{v_{Ci}} \tag{22}$$

when i = chromate and where L represents the height of the ion-exchange bed and v_{Ci} is computed from Eq. 18. Between C_{tran} and C_f, however, all concentration velocities are equal and

$$t_{BC} = \frac{L}{(v_{Ci})_{tran}} \tag{23}$$

Thus, there is an abrupt or sharp transition from C_{tran} to C_f in the effluent history of the column run when mass transfer effects are neglected. Note that for feed concentrations lower than C_{in}, there will be no abrupt transition and breakthrough times (t_{BC}) and bed volumes (BV) for each concentration will be determined by Eqs. 21 and 22.

Experimental Details

Resin

In the original study (Sengupta, 1984), seven different anion-exchange resins were used. However, since the primary goal here is to predict chromate effluent histories, the entire study has been devoted primarily to one commercial anion-exchange resin, IRA-900, which has a polystyrene matrix, divinylbenzene crosslinking, macroporous structure, and a trimethyl quaternary amine (strongly basic) functionality. The IRA-900 resin was obtained from Rohm and Haas Co., but no endorsement is implied and similar resins with equivalent performance are available from other resin manufacturers. From a generic viewpoint, of all the commercial anion-exchange resins studied, resins equivalent to those of IRA-900 showed the highest chromate selectivity and practically negligible oxidative attack by hexavalent chromate. This resin can also be regenerated very efficiently with alkaline brine. Because of the foregoing practical reasons, IRA-900 was chosen for this study. Another anion-exchange resin (IRA-458; polyacrylic matrix, quaternary-amine functionality) was also used in this study primarily to verify the predictive ability of the model. For industrial applications, however, polyacrylic resins are unsuitable due to their relatively low chromate selectivity. The two resins were conditioned following the standard procedure of cyclic exhaustion with 2N hydrochloric acid and regeneration with 2N NaOH. After screening to remove bigger particles and fines, the average size of the spherical beads was 500 ±50 μm. The resins were finally converted to chloride or sulfate forms for batch tests. For the column runs, the resins were presaturated in chloride forms.

Chromate isotherms, column runs, and chemical analyses

The primary objective of this communication, as already indicated, is to present a viable algorithm to predict the effluent history of fixed-bed chromate ion-exchange processes. The experimental procedures for batch isotherm tests, column runs, and chemical analyses have been reported elsewhere by Sengupta and Clifford (1986) and Sengupta et al. (1988) and not repeated here for the sake of brevity.

Results and Discussion

Ternary equilibria

The design constants K_1 and K_2 for chromate-sulfate equilibria were determined for the anion-exchange resin (IRA-900) in accordance with the procedure described in step 1 and using the binary isotherm data generated at the competing sulfate ion concentration of 2,000 mg/L (41.67 meq/L) and 4,000 mg/L (83.3 meq/L). Most of the pertinent isotherm data are presented in Table 1. Similarly, constants K_3 and K_4 were determined for chromate-chloride equilibria at acidic pH using the binary isotherm data, Table 2, for competing chloride concentrations of 2,000 mg/L (56.3 meq/L) and 4,000 mg/L (112.68 meq/L). Resin loadings for the counterions were expressed in meq/g, competing chloride and sulfate ions in meq/L, and the aqueous-phase chromium concentration, Cr(VI), in mg/L. Extremely high chromate separation factors in Table 1 and Table 2 illustrate chromate's very high selectivity over competing sulfate and chloride ions. The following are the computed K values:

$K_1 = 0.0147$ $K_2 = 1.88$ (corr. coeff. = 0.97)

$K_3 = 0.29$ $K_4 = 20.3$ (corr. coeff. = 0.92)

In order to verify the theoretical predictions, chromate distributions were experimentally determined for two sets of ternary

(sulfate-chloride-chromate) equilibria with the following sulfate and chloride concentrations:

Set 1	Set 2
Sulfate 2,000 mg/L	Sulfate 1,000 mg/L
Chloride 1,000 mg/L	Chloride 1,000 mg/L

Figures 4a and 5a show the experimental data points for chromate distributions while the solid lines indicate the predicted chromate distributions calculated in accordance with step 2 of the algorithm using the design constants K_1, K_2, K_3, and K_4 already computed from the binary data. In this step, the nonlinear equations were solved using a Newton-type linearization technique as originally introduced by Shacham and Mah (1978). Both Figures 4a and 5a demonstrate that the shapes and magnitudes of the experimentally determined chromate loadings tally well with the predicted ones, but the experimental values were consistently lower than the predicted ones, especially at higher chromate loadings. Such a difference stems primarily from the assumption that the exchanger-phase activity coefficients, f_{HCr} and f_{Cr2} are independent of the resin composition, which is thermodynamically correct only at very low chromate loadings. Nevertheless, we note that the model, in its present form, can well predict quantitatively the important features of the chromate ion-exchange process. Also, incorporating exchanger-phase activity coefficients in the model as an empirical function of resin composition makes it too complex to be used for predicting column runs for multicomponent systems. That is why models based on separation factors, which consider a constant ratio of the distribution coefficients of counterions between the two phases, have been more frequently applied for dynamic column runs (Helfferich and Klein, 1970; Klein et. al., 1967).

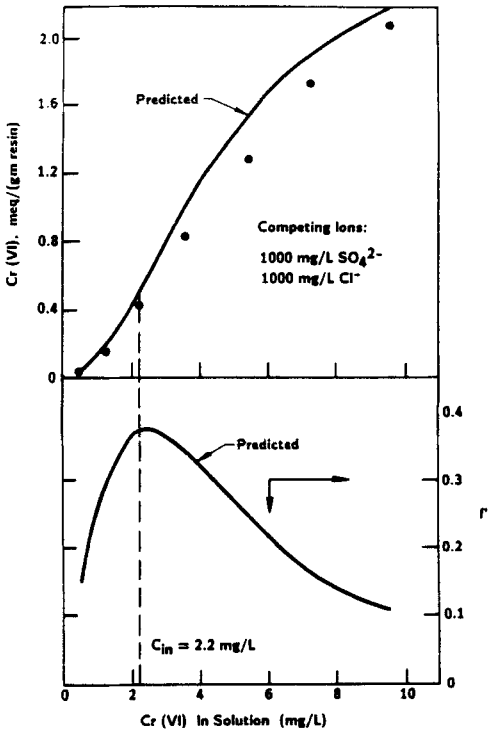

Figure 5. Top, predicted and experimental values of chromate distribution in a ternary system. Bottom, predicted $f'(d\bar{C}/dC)$ vs. aqueous-phase chromate concentration identifying inflection point.

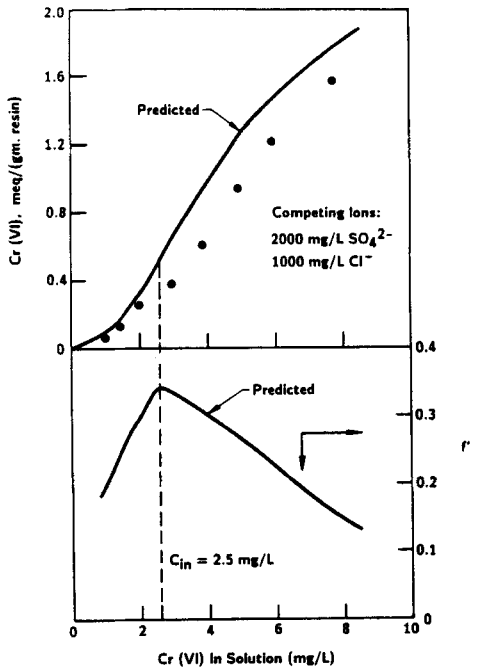

Figure 4. Top, predicted and experimental values of chromate distribution in a ternary system. Bottom, predicted $f'(d\bar{C}/dC)$ vs. aqueous-phase chromate concentration identifying inflection point.

Figures 4b and 5b show how the predicted slopes of the chromate isotherms go through a maximum, indicating the chromate concentrations (C_{in}) corresponding to the inflection points. For the background sulfate and chloride concentrations of the first set, C_{in} corresponds to 2.5 mg/L while C_{in} is 2.2 mg/L for the second set.

Effluent histories

Figure 6 provides the chromate effluent histories of two extremely lengthy column runs that are identical in all respects except for chromate concentrations in the feed. The two feed chromate concentrations were 5.0 and 10.0 mg/L. The competing sulfate and chloride ion concentrations in the feed solutions of these two runs are identical and same as those in ternary equilibria corresponding to Figure 4. For the competing background concentrations of 2,000 mg/L sulfate and 1,000 mg/L chloride, as we have noted in Figure 4, the inflection chromate concentration, C_{in}, is 2.5 mg/L. For both column runs the transition between diffuse and shock waves occurs at concentration less than C_{in}, because feed concentrations (5 and 10 mg/L) are greater than C_{in}.

The following calculations are done to find C_{tran}:

1. At the given feed concentration C_f (5 or 10 mg/L), find $\bar{C}_f$ from algorithm step 2
2. Between zero and C_{in}, pick any chromate concentration

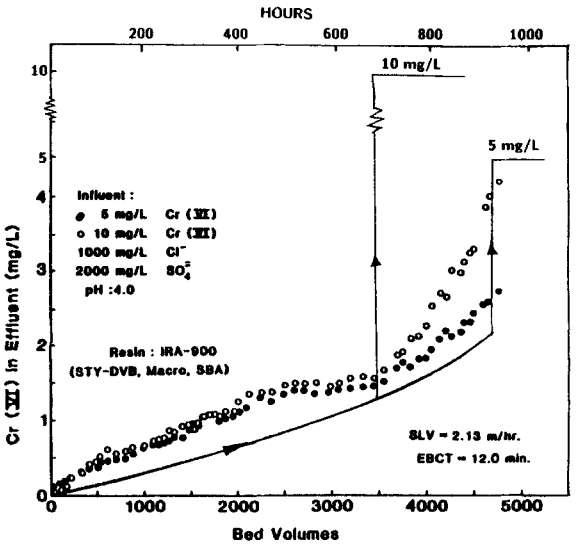

Figure 6. Chromate effluent histories during two fixed-bed column runs in the presence of competing sulfate and chloride anions.

—— Predicted; O O O actual

C_{trial} and find $\overline{C_{trial}}$ and $(\overline{dC}/dC)_{trial}$ using algorithm step 2 and step 3, respectively

3. Continue trial and error until the equality in Eq. 19 of algorithm step 4 is satisfied and $C_{trial} = C_{tran}$.

Obviously, as the feed concentration increases C_{tran} will decrease.

The following C_{tran} concentrations were computed in accordance with the above procedure:

For C_f = 10.0 mg/L, C_{tran} = 1.25 mg/L, and for C_f = 5.0 mg/L, C_{tran} = 2.1 mg/L. For chromate effluent concentrations between zero and C_{tran} (gradual breakthrough), bed volumes of water fed (BV) were determined by Eq. 22 of step 5, while Eq. 23 provided the bed volumes for abrupt breakthrough from C_{tran} through C_f. The solid lines in Figure 6 provide the predicted effluent histories for the two column runs. Although the predicted effluent concentrations are consistently lower than the experimental data during the major part of the column runs, the following key features of the column runs are well verified by the proposed equilibrium model:

- In spite of being highly preferred over chloride and sulfate, chromate breakthrough at acidic pH is very gradual and starts almost immediately after the start of the column runs.
- Although the feed chromate concentration (10 mg/L) in one column run was twice that of the other (5.0 mg/L), the effluent chromate concentrations remained almost identical for both runs for over 3,000 bed volumes of water fed (>600 h), as predicted by the model based on equilibrium chromate ion-exchange mechanism. This is an important feature of fixed-bed chromate ion-exchange processes. If 1.0 mg/L is the maximum allowable chromium concentration in the effluent, both column runs must be terminated at the same time although there remains a significant difference in their feed concentrations.
- The model predicts divergence of the two effluent histories between effluent chromium concentrations of 1.25 and 2.1 mg/L. At approximately 1.7 mg/L of Cr(VI) concentration, the two effluent histories slowly diverge as shown in Figure 6. Obviously in this region of abrupt transition from C_{tran} to C_f, mass transfer limitations will tend to broaden the self-sharpening type breakthroughs. Thus, between effluent chromate concentrations of 1.25 and 2.1 mg/L, the broadening of the concentration wave front for the 10 mg/L feed (open circles) is caused by kinetic limitations while that of 5 mg/L feed (filled circles) is primarily due to the unfavorable equilibrium characteristic. The sharpness in the divergence of the two effluent histories is somewhat obscured. Qualitatively, however, such a divergence can be readily detected in Figure 6.

The fact that the predicted chromate concentrations in the effluent during the gradual breakthrough period are consistently lower than the experimental values, can be adequately explained with the aid of Figure 4a, which shows that the theoretical chromate loadings for ternary equilibria are always slightly greater than the experimental values, primarily due to the assumption that exchanger-phase activity coefficients, f_{HCr} and f_{Cr2}, are independent of the resin composition. Thus, the theoretically predicted derivatives, $\overline{dC}/dC$, is always somewhat higher than the true values and this results in lower concentration velocities for chromate concentrations $<C_{tran}$.

Other feed conditions

The validity of any model is confirmed when it shows the ability to make correct predictions under widely different experimental conditions. To test the generality of the proposed model, data from two more column runs, carried out under somewhat unusual conditions, are presented below.

First, a column run experiment was carried out, as shown in Figure 7a, using a different resin (IRA-458) having a relatively low chromate selectivity compared to IRA-900. Feed chromate concentration was 5.0 mg/L in the presence of 2,000 mg/L competing chloride ions. The chromate isotherm for this anion-exchange resin against the same background concentration of competing chloride ions (2,000 mg/L) is provided in Figure 7b. Numbers in parentheses for each experimental data point indicate its chromate/chloride separation factor, which is always greater than unity. Note that for this resin (IRA-458), the inflection point occurs at a concentration much greater than 5.0 mg/L, that is, this is a situation where feed chromate concentration, C_f, is lower than C_{in}. Thus, the chromate effluent history, according to the prediction of Figure 3, should be gradual up to the end; that is, shock waves will be absent altogether. Note that the effluent chromate history of Figure 7a is in agreement with such a prediction. The solid line in Figure 7a provides the predicted chromate breakthroughs for such a feed condition.

Figure 8 shows a second column run, which was performed with IRA-900 in chloride form where the feed solution contained only 20 mg/L chromate solution at pH = 4.0, that is, no competing ion other than a very small amount of chloride was present and the presence of the chloride ion was due to the addition of HCl to reduce the pH to 4.0. Chromate effluent history in this case, somewhat suprisingly, does not show any gradual breakthrough behavior. No chromate was found in the treated effluent for over 24,000 bed volumes. The following provides the explanation for such a seemingly contradictory behavior: Since the competing ion concentration in this case is extremely low, C_{in} is very close to zero. Therefore, feed chromate concentration C_f is much greater than C_{in} and thus C_{tran} in this case is practically at origin, that is, at zero chromate concentration. In other words, this is an extreme case where only shock wave is pres-

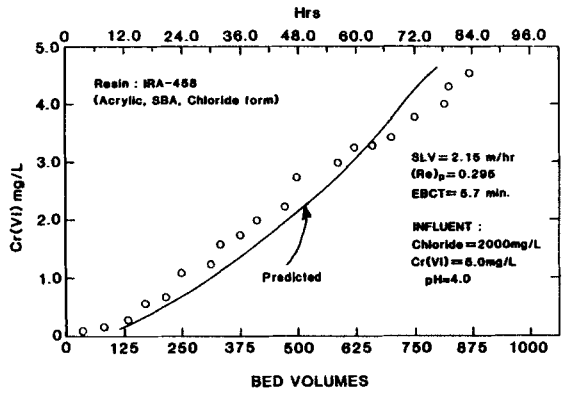

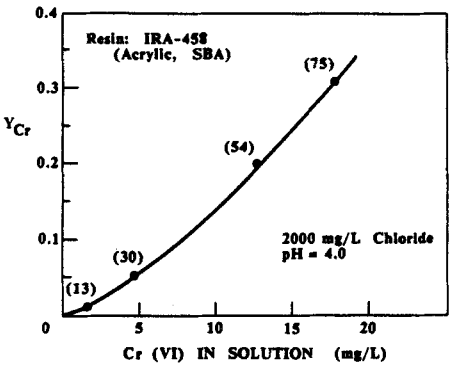

Figure 7a. Chromate effluent history (gradual) for a feed concentration lower than C_{in} in the presence of competing chloride ions.

Figure 7b. Chromate isotherm under conditions of Figure 7a.

ent—the chromate concentration velocities are all equal. From an equilibrium viewpoint, only sharp breakthroughs, as in Figure 8, should occur. Figure 8, therefore, is not in disagreement with the model but in fact confirms its validity under unusual operating conditions.

Conclusions

Due to stringent environmental regulations, the breakthrough of low chromate concentrations (up to 1.0 mg/L) from fixed-bed columns is important in order to assess the operating lengths of the columns runs. The proposed algorithm, based on the governing chromate ion-exchange mechanism, accounts for the unusual features of chromate ion-exchange processes and predicts its column effluent histories fairly accurately in a ternary system. Only binary isotherm data are needed as inputs for this equilibrium model. The model can easily accommodate a multicomponent system with more competing ions. The departure of the model predictions from the experimentally determined column run effluent histories and ternary equilibria may be explained with the aid of simplifying assumptions incorporated in the model. Use of such a model is well justified for chromate ion-exchange processes because constant separation factor models, often used for fixed-bed systems, cannot predict the gradual breakthroughs during column runs for a highly preferred component such as chromate. Molybdates and tungstates tend to behave in a manner similar to chromates due to their ability to form polynuclear species at high concentrations. It is likely that their ion-exchange behaviors can be quantified in a way similar to that developed in this paper for chromate.

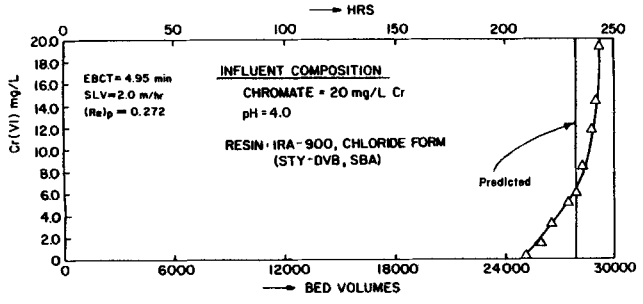

Figure 8. Chromate effluent history (sharp) in the absence of any major competing ion.

Acknowledgment

This work benefited from suggestions by Quiming Yu of Purdue University. The study received partial financial support from the National Science Foundation through Grant No. CBT 8603480.

Notation

C_f = chromate concentration in feed, mg/L
C_i = concentration of species i in liquid phase per unit bed volume, mg/L or meq/L
$\overline{C_i}$ = concentration of species i in exchanger phase per unit bed volume, mg/L or meq/L
C_{in} = chromate concentration at inflection point, mg/L
C_{tran} = chromate concentration at transition between gradual and abrupt breakthroughs, mg/L
$[i]$ = molar concentration of species i in aqueous phase, mol/L
$[\overline{i}]$ = molar concentration of species i in exchanger phase, mol/L or mol/g
I = ionic strength, mol/L
K = equilibrium constant
L = length or height of packed column, m or cm
q_i = concentration of species i per unit g of air-dried exchanger, mg or meq/g resin
Q = total exchange capacity of resin, meq/mL or meq/g
R = fixed organic (benzyl) part of resin
$\overline{RCr_T}$ = exchanger-phase total chromate concentration, mg or mq/g
t = time, h or s
t_{BC} = time at breakthrough for a chromate concentration C, h
v_0 = interstitial liquid velocity in packed bed, m/h or m/s
v_{bulk} = superficial or apparent liquid velocity in packed bed, m/h or m/s
v_{Ci} = concentration velocity of species i at concentration C, m/h
x_i = equivalent fraction of species i in liquid phase
y_i = equivalent fraction of species i in exchanger phase
ϵ = void fraction or porosity of bed
γ_1 = activity coefficient of a monovalent ion in aqueous phase
f_i = activity coefficient of species i in exchanger phase

Abbreviations

SBA = strong base anion
BV = bed volumes
SLV = superficial liquid velocity
Sty-DVB = styrene-divinylbenzene
$(Re)_p$ = particle Reynolds number
EBCT = empty bed contact time

Appendix: Overall Chromate Ion Exchange

Overall chromate exchange needs to be expressed in a manner such that the total exchanger-phase concentration of hexavalent chromium, $\overline{Cr(VI)}$, is given in terms of total aqueous-phase chromate concentration, Cr(VI).

At acidic pH (2–5), in the aqueous phase

$$[\mathrm{Cr(VI)}] = 2[\mathrm{Cr_2O_7^{2-}}] + [\mathrm{HCrO_4^-}] \simeq [\mathrm{HCrO_4^-}] \quad \text{(A1)}$$

[ ] represents molar concentration. At the chromate concentrations (5–20 mg/L) of interest, $Cr_2O_7^{2-}$ is negligible. From Eq. 3 and using Eq. A1

$$[\mathrm{Cr_2O_7^{2-}}] = \frac{K_3}{\gamma_1^2}[\mathrm{Cr(VI)}]^2 \quad \text{(A2)}$$

where K_3 is the thermodynamic equilibrium constant for Eq. 3 and γ_1 is the aqueous-phase activity coefficient of a monovalent ion. The derivation and underlying assumptions for the appearance of the term γ_1 in Eq. A2 is provided by Sengupta and Clifford (1986).

According to the chromate ion-exchange mechanism, the chromate exchange reactions for chromate-sulfate equilibrium may be considered to be taking place with both $HCrO_4^-$ and $Cr_2O_7^{2-}$. Thus for counterion $HCrO_4^-$:

$$\overline{R_2SO_4} + 2\mathrm{HCrO_4^-} \rightleftharpoons 2\overline{R\mathrm{HCrO_4}} + \mathrm{SO_4^{2-}} \quad \text{(A3)}$$

Assuming negligible shrinking/swelling of the exchanger and using the equality of Eq. A1, the thermodynamic equilibrium constant for Eq. A3 is given by

$$K^{I} = \frac{f_{\mathrm{HCr}}^2[\overline{R\mathrm{HCrO_4}}]^2}{f_S[\overline{R_2SO_4}]}\frac{[\mathrm{SO_4^{2-}}]\gamma_1^2}{[\mathrm{Cr(VI)}]^2} \quad \text{(A4)}$$

$$[\overline{R\mathrm{HCrO_4}}] = \left|\frac{K^{I}f_S[\overline{R_2SO_4}]}{[\mathrm{SO_4^{2-}}]}\right|^{1/2}\frac{[\mathrm{Cr(VI)}]}{f_{\mathrm{HCr}}\gamma_1} \quad \text{(A5)}$$

where f_i represents the exchanger-phase activity coefficient for species i and subscripts HCr and S represent $HCrO_4^-$ and SO_4^{2-}, respectively. Similarly, for the counterion $Cr_2O_7^{2-}$:

$$\overline{R_2SO_4} + \mathrm{Cr_2O_7^{2-}} \rightleftharpoons \overline{R_2Cr_2O_7} + \mathrm{SO_4^{2-}} \quad \text{(A6)}$$

After substituting for $[Cr_2O_7^{2-}]$ from Eq. A2, the thermodynamic equilibrium constant for Eq. A6 is given by

$$K^{II} = \frac{f_{\mathrm{Cr2}}[\overline{R_2Cr_2O_7}]}{f_S[\overline{R_2SO_4}]}\frac{[\mathrm{SO_4^{2-}}]\gamma_1^2}{K_3[\mathrm{Cr(VI)}]^2} \quad \text{(A7)}$$

$$\overline{R_2Cr_2O_7} = \frac{K_3K^{II}f_S[R_2SO_4]}{f_{\mathrm{Cr2}}[\mathrm{SO_4^{2-}}]}\frac{[\mathrm{Cr(VI)}]^2}{\gamma_1^2} \quad \text{(A8)}$$

using Eqs. A5 and A8

$$[\overline{RCr_T}] = [\overline{R\mathrm{HCrO_4}}] + 2[\overline{R_2Cr_2O_7}]$$
$$= \left|\frac{K^{I}f_S[\overline{R_2SO_4}]}{[\mathrm{SO_4^{2-}}]}\right|^{1/2}\frac{[\mathrm{Cr(VI)}]}{f_{\mathrm{HCr}}\gamma_1} + \frac{2K_3K^{II}f_S[\overline{R_2SO_4}]}{f_{\mathrm{Cr2}}[\mathrm{SO_4^{2-}}]}\frac{[\mathrm{Cr(VI)}]^2}{\gamma_1^2} \quad \text{(A9)}$$

Equation A9 represents the chromate-sulfate isotherm where the exchanger-phase chromate concentration Cr(VI) is given in terms of the aqueous-phase chromate concentration, Cr(VI), and parameters K_3, K^{I}, K^{II}, f_S, γ_1, f_{HCr}, and f_{Cr2}. Similarly, the chromate-chloride equilibrium at acidic pH is represented by

$$[\overline{RCr_T}] = \frac{K^{I}f_{\mathrm{Cl}}[\overline{RCl}]}{[\mathrm{Cl^-}]f_{\mathrm{HCr}}}[\mathrm{Cr(VI)}] + \frac{2K^{II}K_3f_{\mathrm{Cl}}^2[\overline{RCl}]^2}{f_{\mathrm{Cr2}}[\mathrm{Cl^-}]^2}[\mathrm{Cr(VI)}]^2 \quad \text{(A10)}$$

Equations A9 and A10 represent chromate-sulfate and chromate-chloride equilibrium at acidic pH.

Chromate ion exchange when chromate is a trace species

If chromate is considered to be a trace species in both aqueous and exchanger phases for chromate-sulfate equilibrium, then

$$[\overline{R_2SO_4}] \simeq Q \quad \text{(A11)}$$

$$[\mathrm{SO_4^{2-}}] \simeq C_T \quad \text{(A12)}$$

where Q and C_T are total exchange capacity of the resin and total aqueous-phase concentration, respectively. So, when Cr(VI) is a trace species against a constant background concentration of competing sulfate, C_T is constant. Total exchange capacity, Q, of any particular resin is constant assuming negligible co-ion invasion. Also, chromate being a trace species

$$f_S = 1.0$$

and

$$f_{\mathrm{HCr}},\quad f_{\mathrm{Cr2}} = \text{constant}$$

Thus, all the terms on the righthand side of Eq. A9 become constant except [Cr(VI)].

Equation A9 then takes the following form:

$$[\overline{RCr_T}] = \theta_1[\mathrm{Cr(VI)}] + \theta_2[\mathrm{Cr(VI)}]^2 \quad \text{(A15)}$$

The form of Eq. A15 is also applicable for chromate-chloride equilibrium when chromate is a trace species. Since the equivalent weights of $HCrO_4^-$ and $Cr_2O_7^{2-}$ as Cr are the same, Eq. A15 may be converted into the following form in terms of equivalent fractions:

$$y_{\mathrm{Cr}} = A_1x_{\mathrm{Cr}} + A_2x_{\mathrm{Cr}}^2 \quad \text{(A16)}$$

where A_1 and A_2 are constants and y_{Cr} and x_{Cr} are equivalent chromate fractions in the exchanger phase and aqueous phase, respectively.

Literature Cited

APHA-AWWA-WPCF, "Standard Methods for the Examination of Water and Wastewater," 15th ed., Washington, DC, (1980).

Butler, J. N., *Ionic Equilibrium: A Mathematical Approach*, Addison-Wesley, New York (1967).

Clifford, D., "Multicomponent Ion-exchange Calculations for Selected Ion Separations," *Ind. Eng. Chem. Fundam.*, **21**, 141 (1982).

Golden, F. M., "Theory of Fixed-bed Performance for Ion Exchange Accompanied by Chemical Reaction," Ph.D. diss., Univ. California, Berkeley (1972).

Helfferich, F., *Ion Exchange*, Xerox University Microfilms, Ann Arbor (1961).

Helfferich, F., and G. Klein, *Multicomponent Chromatography: Theory of Interference*, Dekker, Ann Arbor (1970).
Klein, G., D. Tondeur, and T. Vermeulen, "Multicomponent Ion Exchange in Fixed Beds," *Ind. Eng. Chem. Fundam.*, **6**(3), 339 (1967).
Kunin, R., "New Technology for the Recovery of Chromates from Cooling Tower Blowdown," *Amber-Hi-Lites No. 151*, Rohm and Haas, Philadelphia (1976).
Newman, J., and L. Reed, "Weak Base vs. Strong Base Anion-exchange Resins for the Recovery of Chromate from Cooling Tower Blowdown," *AIChE Symp. Ser., Water—1979*, **197**, 76 (1980).
Richardson, E., E. Stobbe, and S. Bernstein, "Ion Exchange Traps Chromates for Reuse," *Environ. Sci. Technol.*, **2**, 1006 (1968).
Sengupta, A. K., "Chromate Ion-exchange Study for Cooling Water," Ph.D. diss. Univ. Houston, TX (1984).
Sengupta, A. K., and D. Clifford, "Chromate-Ion-exchange Mechanism for Cooling Water," *Ind. Eng. Chem. Fundam.*, **25**, 249 (1986).
Sengupta, A. K., S. Subramonian, and D. Clifford, *J. Environ. Eng., ASCE*, (1988).
Shacham, M., and R. S. H. Mah, "A Newton-type Linearization Method for Solution of Nonlinear Equations," *Comput. Chem. Eng.*, **2**, 64 (1978).
Stumm, W., and J. Morgan, *Aquatic Chemistry*, Wiley, New York (1981).
Tondeur, D., and M. Bailly, "Design Methods for Ion-exchange Processes Based on the Equilibrium Theory," *Ion Exchange: Science and Technology*, A. Rodrigues, ed., NATO ASI Ser., M. Nijhoff (1986).
Tong, J., and E. King, "A Spectrophotometric Investigation of the Equilibria Existing in Acidic Solutions of Cr(VI)," *J. Am. Chem. Soc.*, **75**, 6/80 (1953).
Tudge, A., "Studies in Chromatographic Transport," *Can. J. Physics*, **39**, 1611 (1961).
Wang, N.-H. L., and S. Huang, "Multicomponent Ion Exchange in Fixed Beds for Selective Removal of Ammonium Carbonate," *AIChE Symp. Ser. Adsorption and Ion Exchange—83*, **230**, 79 (1984).
Wankat, P. C., *Large-scale Adsorption and Chromatography*, CRC Press, Boca Raton, FL (1985).
Yamamoto, D., Y. Koichi, and Y. Osamu, "Recovery of Chromate from Cooling Tower Blowdown by Ion-exchange Resins," *Proc., Cooling Tower Inst. Meet.*, Houston (1975).
Yu, Q., and N.-H. L. Wang, "Multicomponent Interference Phenomena in Ion Exchange Columns," *Separ. Purif. Meth.*, **15**(2), 127 (1986).

Manuscript received Mar. 7, 1988.